PERGAMON

International Journal of Multiphase Flow 26 (2000) 67–82

International Journal of Multiphase Flow

www.elsevier.com/locate/ijmulflow

The behaviour of gas bubbles in a turbulent liquid metal magnetohydrodynamic flow Part II: Magnetic field influence on the slip ratio

S. Eckert[a,*], G. Gerbeth[a], O. Lielausis[b]

[a]*Forschungszentrum Rossendorf (FZR), 01314 Dresden, P.O. Box 510119, Germany*
[b]*Latvian Academy of Science, Institute of Physics (LAS-IFP), 2169 Salaspils-1, Miera iela 32, Latvia*

Received 5 February 1998; received in revised form 13 January 1999

Abstract

The influence of a steady, homogeneous magnetic field on the slip ratio in a liquid metal bubbly flow is investigated. A one-dimensional model has been developed describing the motion of a multitude of bubbles in a magnetohydrodynamic flow. Calculations are presented for magnetic fields directed transverse or parallel to the mean flow direction. While in the longitudinal case the slip decreases monotonously with the growing magnetic field, it also decreases initially, passes a minimum and increases again if $\vec{B}$ is directed transverse to the flow. In order to validate the theoretical predictions, experiments are performed in liquid metal flows exposed to a transverse or a longitudinal magnetic field.

Keywords: Liquid metal–gas flow; Bubble; Magnetic field; Void fraction; Drag coefficient; Slip ratio; Resistivity probe

1. Introduction

The paper deals with the motion of gas bubbles in a liquid metal exposed to external magnetic fields. While part I of the paper considers the problem of bubble dispersion, in the following part II the momentum transfer from dispersed gas bubbles to the surrounding liquid metal flow is investigated.

Two-phase flows play an important role in a number of technological processes in

* Corresponding author.

0301-9322/00/$ - see front matter
PII: S0301-9322(99)00007-5

metallurgical and chemical industries. Gas bubbles are injected into liquid baths in order to stir liquids (see Szekely (1979) for a review), because often a better homogenisation (temperature or concentration) or the initialisation of a distinct flow structure is desired. In many applications the motion of bubbles in high density fluids, for instance pure liquid metals or alloys, appears. Because of the large differences between the fluid densities, the bubbles are strongly accelerated by the buoyancy force. This results in a higher velocity of the gas particles compared to the liquid phase, in other words the slip ratio S (i.e. gas velocity/liquid velocity) becomes greater than one. However, a high value of the slip S is combined with a considerable loss of kinetic energy. A small slip ratio is desirable for the efficiency of gas bubbles stirring or the concept of liquid metal magnetohydrodynamic (MHD) generators. In the latter case the gas phase is employed as thermodynamic working medium. The gas is injected into a vertical channel in order to transfer kinetic energy towards the liquid metal, which is necessary to drive the flow through the generator section (Branover, 1993; Branover et al., 1988).

Our paper is aimed to look for possibilities allowing to control the slip ratio S in liquid metal–gas two-phase flows by means of external magnetic fields. For a successful employment of such MHD ideas in order to affect the interfacial momentum transfer, the understanding of fundamental flow phenomena is obviously necessary. In general, the numerical analysis of two-phase flows is combined with significant difficulties caused by their complex nature. The main problems arise from the compressibility of the gaseous phase and the deformation of the interfacial area. Therefore, the theoretical handling of two-phase flows is mainly based on empirical laws. For our flow modelling MHD effects have to be taken into account additionally, for which the experimental data base is much smaller compared to the ordinary hydrodynamic case. Therefore, we apply the following strategy: theoretical predictions about the behaviour of the flow are obtained from a simplified one-dimensional model. In parallel, experimental investigations in a broad range of parameters were performed. Comparing the experimental and theoretical results we get an estimate of the employed empirical closure laws of the model and suggest elements for further improvement of the model.

A detailed description of the model can be found in Section 2.1. In Section 2.2 the essential consequences of the magnetic field influence on the slip ratio are demonstrated as resulting from the calculations. Section 3 shows the corresponding experimental results obtained for a transverse and a longitudinal magnetic field configuration, respectively, in comparison with the predictions of the model.

2. Two-phase flow modelling

2.1. Description of the model

Our model is based on the well-known van Wijngarden model of bubbly flow (van Wijngarden, 1972). It is limited to a one-dimensional description of a bubbly flow regime with small gas contents (void fraction $\epsilon < 10\%$). Another model for MHD two-phase flows with arbitrary void fractions based on the two-fluid approach was developed by Thibault (1986). However, this general model is not suitable for a description of the fundamental interfacial processes in terms of single bubble formulations.

We consider a vertical upwards flow of a liquid metal in a rectangular duct exposed to an external magnetic field (Fig. 1). The channel cross section is assumed to be constant. In frame of a one-dimensional analysis all variables enter the code as functions of the coordinate x in flow direction, only, averaged over the cross section. The deviations which arise due to the averaging process can be corrected by means of so-called correlation coefficients as introduced by Yakhot and Branover (1982) or Saito et al. (1978):

$$\overline{\epsilon u_L} = C_1 \bar{\epsilon} \cdot \bar{u}_L. \tag{1}$$

These coefficients have to be determined empirically. However, we refrain from the implementation of the correlation coefficients, because reliable data of the liquid velocities in the entire cross section are not available till now.

The two-phase flow is influenced by a transverse (y-direction) or longitudinal (x-direction) magnetic field. According to the experimental conditions the field strength can be assumed to be constant in the field region, but end effects are also taken into consideration. In the end regions the magnetic field decreases exponentially. The induced magnetic field can be neglected since the condition of a very small magnetic Reynolds number Rm is normally fulfilled under laboratory conditions. Particularly for the MHD generator case the channel side walls are considered as electrodes with an ideal electrical conductivity. For this case, the electric current density $\vec{j}$ as well as the induced electric field $\vec{E}$ ($\vec{j} = \sigma_{el}(\vec{E} + \vec{u} \times \vec{B})$, σ_{el} is the electrical conductivity) has only one component in z-direction. From $\nabla \cdot \vec{E} = 0$ and $\nabla \times \vec{E} = 0$ follows the spatial homogeneity of $\vec{E}$. Nevertheless, in frame of our model also channel configurations with an arbitrary wall conductivity can be treated.

The model is founded on the following assumptions:

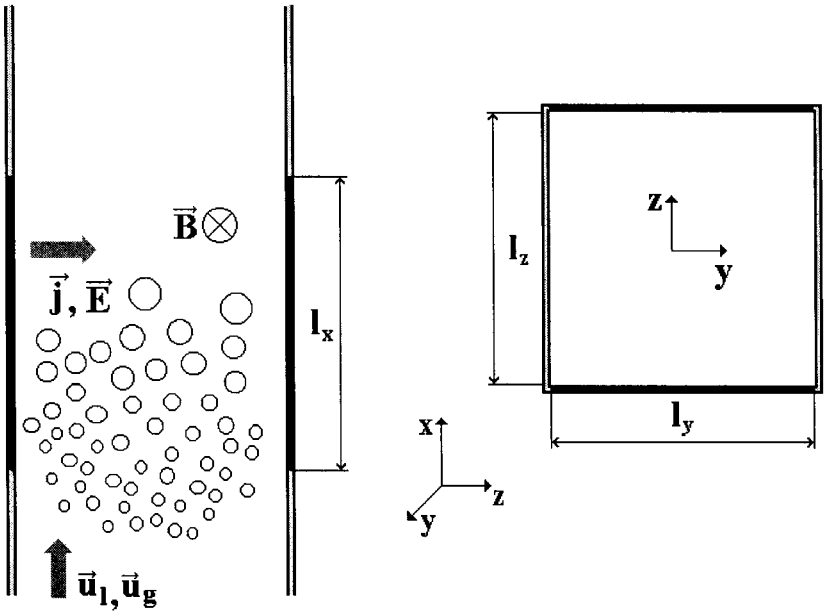

Fig. 1. Simplified sketch of a vertical, rectangular MHD channel considered in the model.

- The flow is isothermal due to the large heat capacity of the liquid metal.
- The flow is steady and fully developed.
- The pressure difference between the gas inside the bubble and the surrounding liquid is negligible.
- The gas phase is treated as ideal gas.
- The gas phase consists of spherical bubbles with a mean radius $r(x)$.
- There is no mass transfer between the phases (i.e. no evaporation or condensation).
- The bubble number is assumed to be constant (i.e. no aggregation or breakup of bubbles).

Starting with these assumptions we obtain the final system of equations with the following notations: u_L,u_G are the velocities (the indices L and G denote the liquid and the gas phase), ϵ is the void-fraction, p is the pressure, r is the bubble radius, ρ_G is the density of the gas and g is the gravitational acceleration:

Conservation of mass:

$$\frac{\mathrm{d}\left[(1-\epsilon)u_L\right]}{\mathrm{d}x} = 0 \qquad \frac{\mathrm{d}[\epsilon\rho_G u_G]}{\mathrm{d}x} = 0. \tag{2}$$

Momentum transport:

$$\epsilon\rho_G u_G\left(\frac{\mathrm{d}u_G}{\mathrm{d}x}\right) + (1-\epsilon)\rho_L u_L\left(\frac{\mathrm{d}u_L}{\mathrm{d}x}\right) = -\frac{\mathrm{d}p}{\mathrm{d}x} - \left[\epsilon\rho_G + (1-\epsilon)\rho_L\right]g - f_R + f_{Lo} \tag{3}$$

where $f_{Lo} = (\vec{j}\times\vec{B})_x = \sigma_{el,tp} u_L B_0^2[1-K(x)]$ is the Lorentz force density.

Equation of motion of a single bubble (*with V_b as bubble volume*):

$$\frac{\mathrm{d}\left(\rho_G V_b u_G\right)}{\mathrm{d}t} = -V_b\frac{\mathrm{d}p}{\mathrm{d}x} - \rho_G V_b g - \mathrm{F_D} - F_{VM} \tag{4}$$

where $F_D = 0.5\rho_L\pi r^2 C_D(u_G-u_L)|\,u_G-u_L\,|$ is the drag force and $F_{VM} = 0.5\rho_L u_G(\mathrm{d}[V_b(u_G-u_L)])/\mathrm{d}x)$ is the virtual mass force.

Bubbles mass conservation and equation of state:

$$\rho_G r^3 = \text{const.}, \qquad \frac{p}{\rho_G} = \text{const.} \tag{5}$$

This system of equations is completed by adding the corresponding closure laws for the frictional force density f_R, the apparent electrical conductivity of the two-phase flow $\sigma_{el,tp}$, the load factor $K(x)$ and the bubble drag coefficient C_D. The empirical closure relations are implemented in the code as follows:

- The value of f_R is specified according to a Lockhart–Martinelli modelling (Storek and Brauer, 1980)
- The two-phase electrical conductivity depends only on the void fraction ϵ (Tanatugu et al., 1972). In the code this is optionally realized by

(a) Maxwell's theoretical relation for small ϵ

$$\sigma_{\mathrm{el,tp}} = \sigma_{\mathrm{el,L}} \frac{2(1-\epsilon)}{2+\epsilon} \tag{6}$$

(b) the empirical relation of Petrick and Lee (1964)

$$\sigma_{\mathrm{el,tp}} = \sigma_{\mathrm{el,L}} \exp(-3.8\epsilon) \tag{7}$$

- In order to obtain a formulation of the Lorentz force term included in the Navier–Stokes equation, it is suitable to introduce the load factor $K(x)$. The current density is generally given by Ohms law

$$j_z = \sigma_{\mathrm{el,tp}}(E_z + u_{\mathrm{L}} B_0) \tag{8}$$

($j_z > 0$ MHD generator, $j_z < 0$ MHD pump). Eq. (8) can then be rewritten as

$$j_z = \sigma_{\mathrm{el,tp}} u_{\mathrm{L}} B_0 \big[1 - K(x)\big] \tag{9}$$

where the definition of K is given by $K(x) = -(E_z/u_{\mathrm{L}}B_0)$. The voltage between the electrodes results from

$$U_{\mathrm{e}} = -\int_{-l_z/2}^{l_z/2} E_z \,\mathrm{d}z = -E_z l_z \tag{10}$$

and the total current can be calculated from

$$I = \int_0^{l_x} \int_{l_y/2}^{l_y 2} j_z(x) \,\mathrm{d}x \,\mathrm{d}y. \tag{11}$$

The voltage can further be written as $U_{\mathrm{e}} = IR_{\mathrm{ext}}$, where R_{ext} represents the external electric resistance of the MHD channel. The constancy of E_z makes it meaningful to introduce the initial load factor K_0

$$K_0 = K(x) \frac{u_{\mathrm{L}}}{u_{\mathrm{L}(x=0)}} = \frac{U_{\mathrm{e}}}{u_{\mathrm{L}(x=0)} B_0 l_z} = \frac{IR_{\mathrm{ext}}}{u_{\mathrm{L}(x=0)} B_0 l_z}. \tag{12}$$

For the Lorentz force term we finally obtain

$$\left(\vec{j} \times \vec{B}\right)_x = -\sigma_{\mathrm{el,tp}} B_0^2 \big(u_{\mathrm{L}} - K_0 u_{\mathrm{L}(x=0)}\big). \tag{13}$$

- To describe the motion of a multitude of bubbles the bubble drag coefficient has to be modified. The drag coefficient C_{D} of a bubble in a swarm can be related to the drag coefficient C_{Ds} of a single bubble moving in an infinitely extended liquid bath according to an empirical law found by Mond and Sukoriansky (1985)

$$C_{\mathrm{D}} = C_{\mathrm{Ds}} (1-\epsilon)^4. \tag{14}$$

Now the influence of the magnetic field on the single bubble drag has to be modelled. The

crucial parameters are the Reynolds number $Re_b = |u_G - u_L| d_b/\nu$ (ν is the kinematic fluid viscosity) and the Stuart number $N_b = \sigma_{el} B_0^2 d_b/[\rho_L |u_G - u_L|]$. The subscript b stands for bubble and indicates the use of the bubble diameter d_b and the velocity difference between gas and fluid as characteristic scales. Empirical relations for MHD drag coefficients of spherical bodies are summarized in the monograph of Gelfgat et al. (1976)

$$C_{Ds} = C\left(1 + 0.7\sqrt{N_b}\right) \quad \left(10^3 \le Re_b \le 8.6 \times 10^3,\ 0 \le N_b \le 1.5\right) \tag{15}$$

$$C_{Ds} = C\left(1 + \sqrt{N_b}\right) \quad \left(20 \le Re_b \le 5 \times 10^2,\ 0 \le N_b \le 2.3 \times 10^3\right) \tag{16}$$

in the case of a transverse field $\vec{B} = B_0 \vec{e}_y$, and

$$C_{Ds} = 0.33\sqrt{N_b} \quad \left(10^3 \le Re_b \le 2.5 \times 10^5,\ 10 \le N_b \le 80\right) \tag{17}$$

in the case of a longitudinal field $\vec{B} = B_0 \vec{e}_x$. Here C denotes the drag coefficient of a single bubble without magnetic field as a function of the Reynolds number Re_b, taken here as the standard drag curve (see Clift et al., 1978).

The MHD channel can be characterized by an equivalent electric scheme shown in Fig. 2. The section works as a d.c. source (source voltage U_{oc}, internal resistance R_{int}) connected with the external resistance R_{ext} given by the following equation:

$$\frac{1}{R_{ext}} = \frac{1}{R_E} + \frac{1}{R_{Ha}} + \frac{1}{R_C + (R_{Ld} R_W / R_{Ld} + R_W)} \tag{18}$$

(with load resistance R_{Ld}, wall resistance R_W, end resistance R_E, resistance of the Hartmann-layers R_{Ha} and resistance of the connection between liquid metal and channel wall R_C).

In the generator case the load resistance R_{Ld} can be considered as very low in the sense $R_{Ld} \ll R_W, R_E, R_{Ha}$. That means for a negligible contact resistance R_C the external resistance is identical with the load resistance. If the channel is not connected with an outer electric circuit ($R_{Ld} \to \infty$), the closure of the electric current occurs in the Hartmann layers as well as in the channel wall.

End effects were taken into account according to the findings of Sutton et al. (1962). In the

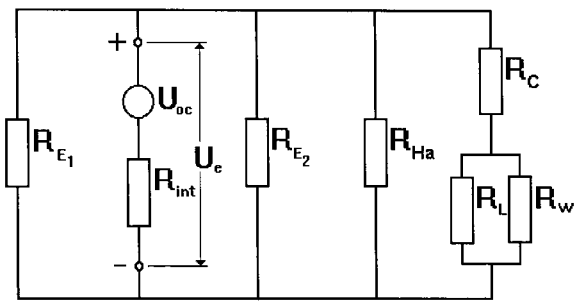

Fig. 2. Equivalent electrical circuit of an MHD channel.

end regions of the magnet the electrically conducting fluid acts as an electric shunt R_E parallel to the fluid domain inside the homogeneous field. So, R_E can be written as (Sutton et al., 1962)

$$R_E = \frac{\pi}{\sigma_{el,tp} l_y (\ln 2 - \zeta)} \tag{19}$$

where

$$\zeta = \gamma^{-1}\left[1 - \pi^{-1/2}\frac{\Gamma(0.5\gamma + 0.5)}{\Gamma(0.5\gamma + 1)}\right]$$

$$\gamma = \frac{l_y}{\pi x_e} \quad \left(l_y \text{ is the channel extension in magnetic field direction}\right).$$

where the fringe field regions of $\vec{B}$ are described by $B = B_0 \exp(-[|x| - x_0]/x_e)$ (x_0 is begin of the homogeneous magnetic field region and x_e is the characteristic decay length of the magnetic field). Obviously, R_E consists of two parts arising from inlet and outlet of the magnetic field, respectively.

2.2. Main theoretical results

Our interest is focused on the dependence of the slip ratio $S(x) = u_G/u_L$ on the external magnetic field. Fig. 3 shows a typical numerical result obtained for a sodium–argon flow exposed to a transverse and a longitudinal magnetic field, respectively.

In the case of a transverse magnetic field, two opposite effects can be noticed:

- The Lorentz force $\vec{f}_{Lo} = \vec{j} \times \vec{B} \sim B^2$ is responsible for an overall braking of the liquid metal flow leading to an increase of S for increasing magnetic field.

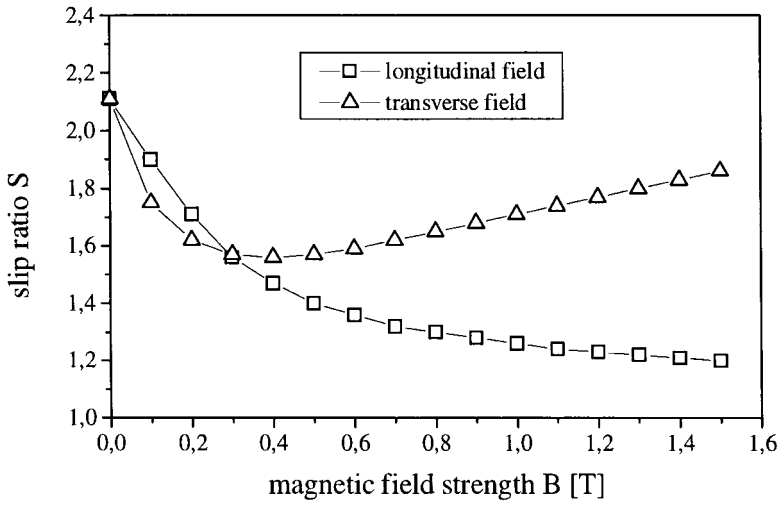

Fig. 3. Representative results of the calculations obtained for a sodium–argon flow ($Re = 27900$).

- The applied magnetic field gives rise to an enhancement of the drag coefficient of a single bubble leading to a decrease of S for increasing magnetic field. According to the relations (15) and (16) this effect is characterized by a linear dependence on B.

Both tendencies are reflected in the shape of the curve in Fig. 3. For small values of the field strength the variations of the slip ratio are mainly influenced by the increasing drag coefficient, whereas for larger field strengths the electromagnetic braking of the mean flow dominates. Therefore, in the first part of the curve the slip ratio decreases with increasing B, reaches a minimum and grows again with further increase of the field strength.

A complete different situation was found if the magnetic field is aligned with the mean flow direction. Here, the first effect of an overall liquid metal braking almost all disappears due to $\vec{u}_L \times \vec{B} = 0$. As a result, we observe a monotonous decrease of the slip ratio with increasing magnetic field.

3. Void fraction measurements

3.1. Experimental setup and data analysis

Experimental investigations have been performed at the FZR sodium facility and at the mercury facility of the Institute of Physics of the Latvian Academy of Science (IfP-LAS) in Riga. While the sodium loop in Rossendorf is equipped with a transverse magnetic field, investigations with a longitudinal field are possible at the IfP facility.

A detailed description of the experimental loops has already been given in part I of this paper (Eckert et al., 2000). In both cases the gas phase is injected through a single orifice into a vertical upwards liquid metal flow. Before the flow leaves the homogeneous region of the applied magnetic field the local void fraction ϵ is measured by single-wire potential probes at discrete points in the cross-sectional area A. A continuous function for ϵ between these positions is determined by interpolation. With the assumption of temporal steadiness, we get the cross-sectional averaged void fraction $\epsilon(x)$ by integration

$$\epsilon(x) = \frac{1}{A}\int_A \epsilon\left(x,y',z'\right)\,\mathrm{d}y'\,\mathrm{d}z'. \tag{20}$$

Eventually, the slip ratio $S(x)$ can be expressed as a function of the void fraction ϵ and the volumetric quality β (where $\dot{Q}_L$ and $\dot{Q}_G$ are the volumetric flow rates of the liquid and the gas, respectively):

$$S(x) = \frac{\beta\left[1-\epsilon(x)\right]}{\epsilon(x)\left[1-\beta\right]}, \qquad \left(\beta = \frac{\dot{Q}_G}{\dot{Q}_L + \dot{Q}_G}\right). \tag{21}$$

The flow characteristics expected for both experimental configurations have been intensively discussed in part I of this paper. Especially, the typical size and the shape of the injected bubbles has been estimated. In this context, we expect to get bubbles with a mean diameter of about 7 mm in the sodium facility as well as in the mercury experiment at gas flow rates of

about 30 l/h. In contrast to the model assumptions, spherical bubbles exist in both experiments only at very small gas flow rates. However, to keep the measuring time and the statistical error of the measurements in a reasonable limit we accept this deviation from the ideal spherical shape.

3.2. Transverse magnetic field

The configuration of a transverse magnetic field has been investigated at the FZR sodium loop. The mean sodium velocity is varied between 0.1 and 0.5 m/s equivalent to Reynolds numbers of 9300 and 46500, respectively.

The experimental results of the void fraction ϵ and the corresponding slip ratio S are shown as functions of the magnetic field strength in Figs. 4–6. The diagrams also contain the direct comparison of the experimental findings with the calculated curves for the slip ratio at the probe position obtained from the model. In view of the simple one-dimensional character of the model the agreement can be considered as satisfactory. The predicted tendency for a decreasing slip when the magnetic field strength grows is clearly confirmed by the experiment. Concerning the low liquid velocities considered in Figs. 4 and 5, minimum of the slip ratio has to be expected for magnetic fields $B > 0.5$ T which cannot be realized with our electromagnet. With increasing sodium velocity this minimum is shifted towards smaller values of the field strength. Indeed, a slight re-enhancement of the slip ratio is observed in Fig. 6 for a mean sodium velocity of 0.5 m/s.

Compared to the measured mean void fractions our bubbly flow model overestimates the void fraction ϵ at $\vec{B} = 0$ and underestimates ϵ if $\vec{B} \neq 0$. The reason is the restriction of the model to one dimension. In the one-dimensional description naturally a uniform distribution of all flow quantities over the channel cross section is assumed, or in other words the distribution

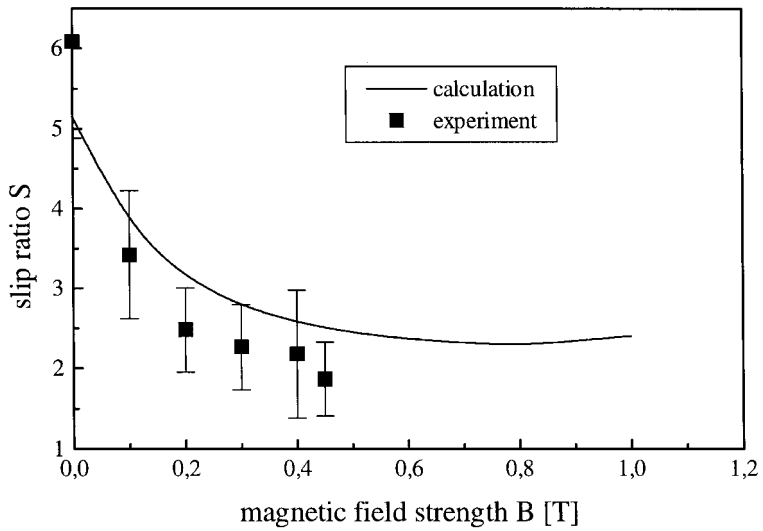

Fig. 4. Comparison of numerical and experimental results for the slip ratio S as a function of the field strength B ($Re = 9300$, transverse magnetic field).

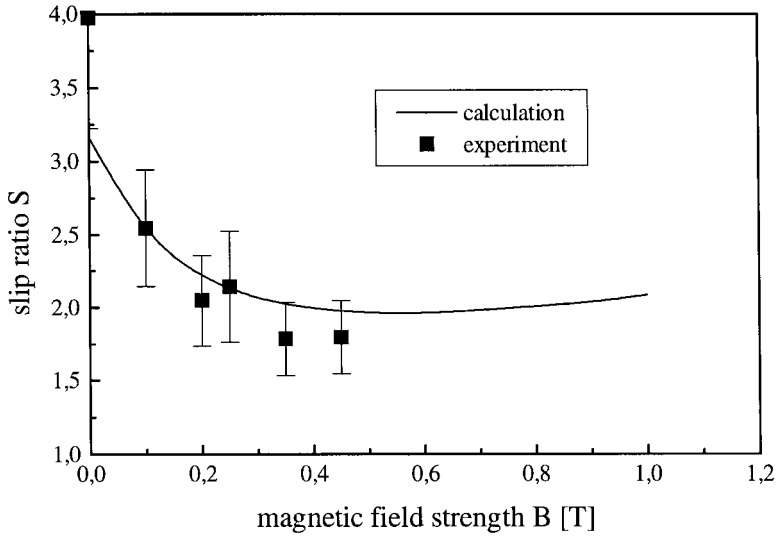

Fig. 5. Comparison of numerical and experimental results for the slip ratio S as a function of the field strength B ($Re = 18600$, transverse magnetic field).

parameter introduced in the drift flux model by Zuber and Findlay (1965) is unity. In general, this condition is not fulfilled in the experiment. The profiles of the local void fraction and the sodium velocity are strongly affected by the external magnetic field. As already shown in part I (Eckert et al., 2000), an essential feature of turbulent MHD flows is the electromagnetic

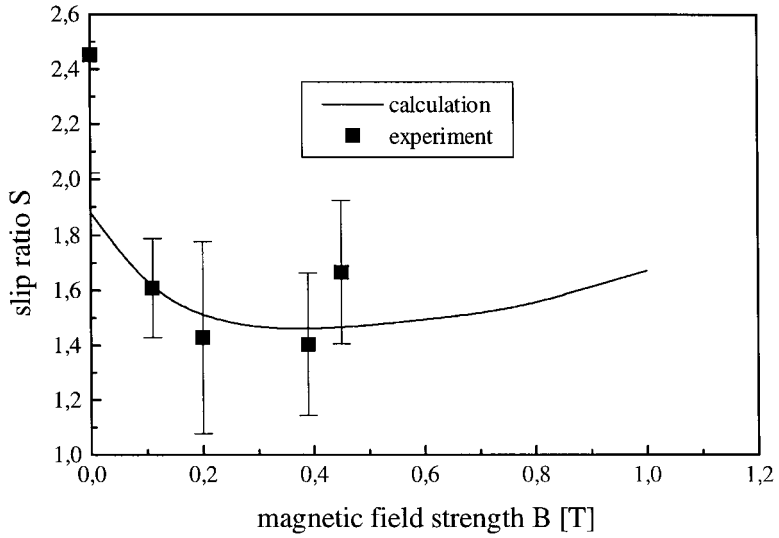

Fig. 6. Comparison of numerical and experimental results for the slip ratio S as a function of the field strength B ($Re = 46500$, transverse magnetic field).

damping of the velocity fluctuations by the Lorentz force. This results in a concentration of the gas bubbles in the channel centre. Simultaneously, a serious reorganization of the velocity field takes place. While in the case $\vec{B} = 0$ an ordinary turbulent channel flow can be expected, the velocity profile is flattened by the magnetic field. Moreover, at higher values of the field strength the velocity profile becomes M-shaped, i.e. in the core of the flow one will find a lower velocity compared to the side walls parallel to the field direction (see also Moreau, 1990). In the MHD situation with an M-shaped velocity profile and a concentration of the gas bubbles in the channel centre the model will inevitable underestimate the void fraction, whereas in the ordinary hydrodynamic case it has the tendency to overestimate ϵ.

In addition to the void fraction ϵ, the bubble velocities have also been measured by means of double-wire resistivity probes. The data have been acquired with a sensor fixed in the channel centre 290 mm behind the point of gas injection. The results shown in Fig. 7 generally confirm the void fraction measurements by means of the single-wire probes. The bubble velocity decreases with growing magnetic field strength. The rise of the gas velocity for a B-field of 0.45 T in the case of $\bar{u}_L = 0.2$ m/s is likely be caused by the reduction of the local drag coefficient due to the concentration of the gas bubbles in the centre of the cross section.

A qualitative confirmation of our numerical results in the case of a transverse magnetic field was also reported by Thibault and Mihalache (1997). The authors investigated a mercury–air flow and found a minimum of the slip ratio at magnetic field strengths of 0.4–0.5 T. However, there is a difference between model and experiment in the absolute values of the slip ratio of about 50%. The reason for this deviation are the high gas flow rates chosen in these experiments. While the theoretical modelling is based on a bubbly flow, a churn flow regime was observed in the experiment requiring a different empirical approach for the drag coefficient as used in our model.

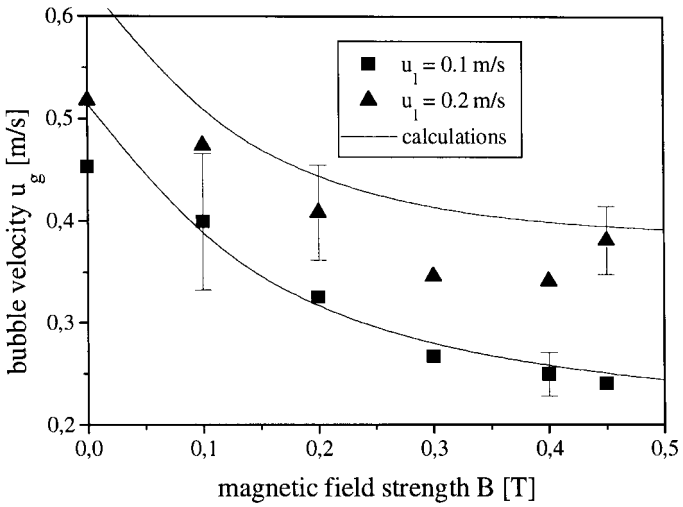

Fig. 7. Bubble velocities obtained by means of double wire resistivity probes in the centre of the channel cross section for two different mean liquid velocities (transverse magnetic field).

3.3. Longitudinal magnetic field

The effect of an external magnetic field aligned with the mean flow direction on the slip ratio was studied in a mercury–nitrogen bubbly flow. Reynolds numbers up to 163000 correspond to a maximum inlet velocity of 0.18 m/s.

The local void fraction is again determined by means of single-wire resistivity probes. Sixteen individual probes are mounted at a cross-shaped frame in such a manner that every sensor is installed at a different radial distance from the centre of the channel cross section. This frame can be rotated as well as translated in axial direction.

Unfortunately, in the actual case our intention to compare the model predictions with the corresponding experimental results is faced with the fact that the validity of the empirical relation implemented in the model for the calculation of the drag coefficient (Eq. (17)) is limited to the range $10 \leq N_b \leq 80$. However, as can be seen in Table 1, where some essential parameters of the sodium and the mercury experiment are compared, the maximum value for N_b in the IfP experiments reaches the order of one, only. To be able to perform calculations in the parameter range $0 \leq N_b \leq 10$, we interpolate the dependence of the bubble drag coefficient on the Stuart number N_b by a third-order polynom (see Fig. 8), thus fitting the original data of Yonas (1967) with sufficient accuracy. First of all it can be concluded that the electromagnetic forces should be obviously too weak to influence the drag balance drastically at $N_b \approx 1, \ldots, 2$, and therefore remarkable changes of the slip ratio cannot be expected.

Satyamurthy et al. (1997) measured the mean void fraction non-intrusive by means of gamma-ray attenuation method in a mercury–nitrogen pipe flow which was exposed to a longitudinal magnetic field up to 0.25 T. The maximal value of the interaction parameter N_b was approximately 0.2. The observed change in the cross-sectional averaged void fraction the authors intended to detect was within the experimental errors, thus confirming our prediction.

Fig. 9 shows the comparison of our experimental results with the calculations regarding the void fraction as well as the slip ratio as a function of the magnetic field strength B. In contrast to the theoretical results, the experiment reveals an increase of the slip ratio with increasing magnetic field.

Looking for a reason of this discrepancy at first the question may arise whether the complete neglect of the Lorentz force term in the model is permissible. A number of papers dealing with

Table 1
Comparison between a Na/Ar and a Hg/N_2 flow regarding some selected physical properties and dimensionless parameters ($d_b = 7$ mm)

Fluid	Hg/N_2 (IfP Riga)	Na/Ar (FZR)
Temperature (°C)	20	200
ρ_L (kg/m^3)	1.36×10^4	9.03×10^2
$\sigma_{el,L}$ (1/Ωm)	1.0×10^6	7.46×10^6
Re_b number	14200	3550
Ha_b number	≤ 150	≤ 400
N_b number	≤ 1.8	≤ 45

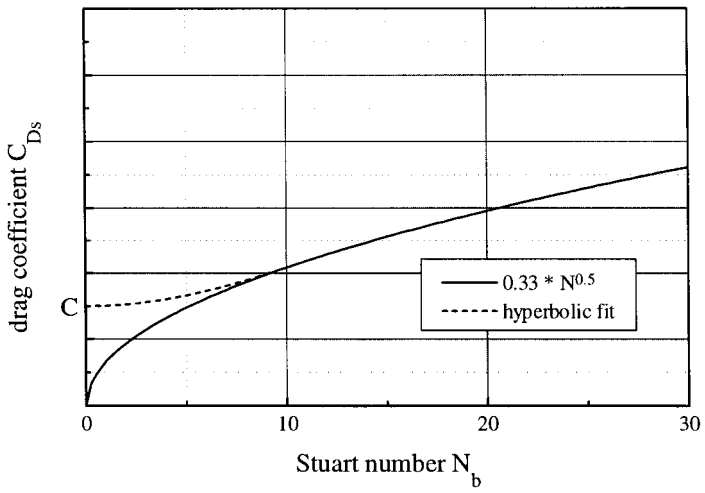

Fig. 8. Empirical relation for the bubble drag coefficient in the case of a longitudinal magnetic field (from Gelfgat et al., 1976) and the used fit for the region of small interaction parameters ($N_b < 10$).

liquid metal duct flow in a longitudinal magnetic field were reviewed by Lielausis (1975). In fact, considering a laminar flow there is no interaction between mean flow and magnetic field ($\vec{u} \times \vec{B} = 0$) and the skin friction factor coincides with the ordinary Poiseulle law. In a turbulent flow the velocity fluctuations are affected by the Lorentz force. However, a rough estimate by means of an empirical relation suggested by Krasilnikov et al. (see Lielausis, 1975) shows a rather small influence of this turbulence damping effect on the skin friction factor at moderate Hartmann numbers $Ha = B_0 L\sqrt{\sigma_{el}/\rho\nu}$:

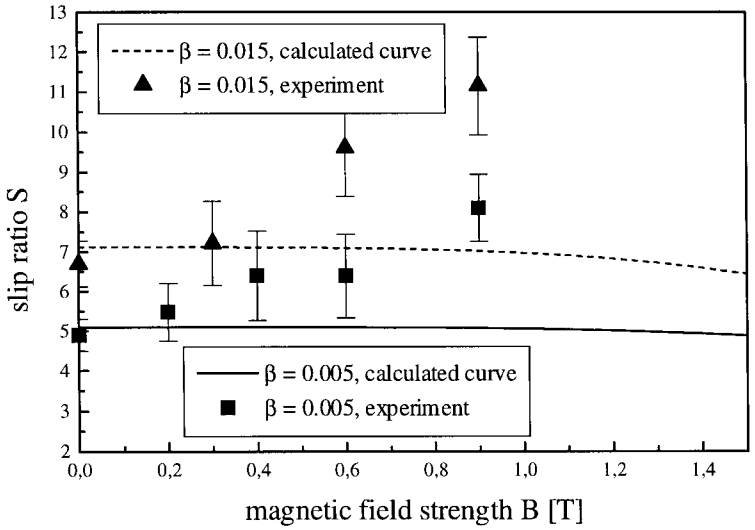

Fig. 9. Comparison of numerical and experimental results for the slip ratio S as a function of the field strength B ($Re = 81600$, longitudinal magnetic field).

$$\lambda = \lambda_0 \left[1 - 1.85 \cdot \left(\frac{Ha}{Re} \right)^{1.6} \right] \quad 0 < Ha/Re \leq 4 \times 10^{-2} \tag{22}$$

where λ_0 is the skin friction factor in the case $B = 0$.

The skin friction is reduced by the action of the magnetic field, i.e. this effect alone would result in a decrease of the slip ratio. Moreover, in our experiment the maximum field strength of 0.9 T corresponds to a Hartmann number of 2320 leading to values up to 0.03 for the ratio Ha/Re and always less than 0.01 for the right-hand term in Eq. (22), respectively, i.e. this effect is not relevant for the measured results.

To find a possible explanation for the difference between experimental and theoretical results we also have to look at the local characteristics of the flow. Mori et al. (1977) investigated rising bubbles in a mercury tank exposed to a horizontal magnetic field using a triple-wire resistivity probe. They reported an enhancement of the vertical terminal velocity caused by the application of the field, if the bubble sizes are not too large. As reason for this behaviour they found the transformation of the typical spiral rise of the bubbles into a rectilinear movement. In the case of a longitudinal magnetic field a similar effect can be expected, resulting in an increase of the slip ratio with increasing magnetic field strength as observed in our experiment. Obviously, this effect is not included in our simplified one-dimensional model.

In view of the large magnetic field length (the solenoid at IfP has a length of 2 m) a considerable influence arising from end effects of the $\vec{B}$-field on the void fraction measurements cannot be identified. The strength of the fringe field in the end region was assessed and implemented into the code. The numerical results show that detectable changes of the mean velocity appear only in the fringe field regions, thus having almost no influence on the measured slip ratio in the homogeneous field region.

Another point of discussion is a possible modification of the flow by the presence of a local sensor. We consider a uniform flow of an electrically conducting fluid in a longitudinal magnetic field disturbed by a cylinder with the axis parallel to the flow direction. In addition to the well-known viscous wake, in the MHD case two magnetic wakes parallel to the applied field lines arise, where the flow is disturbed considerably. The reason is the propagation of Alfven waves originating at the cylinder (see Moreau, 1990). Because in our experiment the Alfven velocity $v_A = B/\sqrt{\rho \cdot \mu_0}$ is much higher than the velocity of the mean flow, the flow is already slightly perturbated upstream of the obstacle. That means, a possible deflection of the rising bubbles from the probe axis cannot be excluded. The influence of such an effect on the void fraction measurements should be taken into account by further investigations.

4. Conclusions

In order to describe the behaviour of an MHD two-phase flow a one-dimensional model for the bubbly flow regime was developed. The closure of the system of equations has been done by the inclusion of empirical laws. The model provides basic information and tendencies about the dependence of the slip ratio S on the applied magnetic field.

Two opposite tendencies were observed in the case of a transverse field. On the one hand, the drag coefficient of a single bubble grows linearly with increasing field strength B. On the

other hand, the electromagnetic braking of the mean flow has to be taken into consideration. The Lorentz force term is proportional to B^2. Thus, at first the slip ratio decreases in the range of small field values, reaches a minimum and increases again for a further growth of B. The application of a longitudinal magnetic field causes also an enhancement of the bubble drag coefficient. In contrary to the transverse case the Lorentz braking effect almost disappears. Consequently, we obtain a continuously decreasing slip ratio with increasing field strength.

The theoretical predictions for the application of a transverse field were qualitatively confirmed by measurements in a sodium–argon flow. The deviations between experimental and theoretical results are caused by the limitations of our one-dimensional modelling. Experiments performed with a longitudinal magnetic field in a mercury–nitrogen flow show a disagreement with the predictions of the model. We conclude that the interaction of the longitudinal magnetic field with the turbulent fluctuations may be responsible for this discrepancy, causing a more rectilinear motion of the bubbles compared to its usual helical or zig-zag motion without magnetic field. This effect as well as the influence arising from perturbations of the flow structure caused by the presence of local sensors in the MHD flow should be investigated in more detail in further work.

Acknowledgements

This work was supported by the Deutsche Forschungsgemeinschaft under contract Ge 682/4-1. Furthermore, the authors would like to express their thanks to H. Langenbrunner, W. Witke, Y. Kolesnikov and E. Platacis for their valueable support in preparing and performing the experiments at both liquid metal facilities in Rossendorf and Riga, respectively.

References

Branover, H., 1993. Liquid-metal MHD research and development in Israel. In: Proceedings of the Sixth Beer-Sheva Seminar, Jerusalem, 1990. AIAA 148, 209–221.

Branover, H., El-Boher, A., Lesin, S., Unger, Y., 1988. Testing of OMACON-type MHD power systems. In: Proceedings of the Sixth Beer-Sheva Seminar, Jerusalem, 1987. AIAA 111, 209–229.

Clift, R., Grace, J.R., Weber, M.E., 1978. Bubbles, Drops and Particles. Academic Press, New York.

Eckert, S., Gerbeth, G., Lielausis, O., 2000. The behaviour of gas bubbles in a turbulent liquid metal magnetohydrodynamic flow. Part I: Dispersion in quasi-two-dimensional magnetohydrodynamic turbulence. Int. J. Multiphase Flow 26, 45–66.

Gelfgat, Y.M., Lielausis, O.A., Sherbinin, E.W., 1976. Liquid metals under the action of electromagnetic fields. Zinatne, Riga.

Lielausis, O.A., 1975. Liquid-metal magnetohydrodynamics. Atomic Energy Review 13, 527–581.

Mond, M., Sukoriansky, S., 1985. An analytical model for bubbly flow. In: Proceedings of the Fourth Beer-Sheva Seminar, Jerusalem, 1984. AIAA 100, 329–339.

Moreau, R., 1990. Magnetohydrodynamics. Kluwer, Dordrecht, Boston.

Mori, Y., Hijikata, K., Kuriyama, I., 1977. Experimental study of bubble motion in mercury with and without magnetic field. J. Heat Transfer (Trans. ASME) 99, 404–410.

Petrick, M., Lee, K.Y., 1964. In: Proceedings of the Second International Symposium on MHD Electrical Power Generation, vol. 2, Paris.

Saito, M., Inoue, S., Fujii-E, Y., 1978. Gas-liquid slip ratio and MHD pressure drop in two-phase liquid metal flow in strong magnetic field. J. Nucl. Sci. Technol 15, 476–489.

Satyamurthy, P., Dixit, N.S., Thiyagarajan, T.K., Grover, R., Demello, M., Venkatramani, N., 1997. Effect of longitudinal magnetic field on void fraction profiles in the riser of a liquid metal MHD energy conversion system of gravity type. In: Proceedings of the Third International Conference on Transfer Phenomena in Magnetohydrodynamic and Electroconducting Flows, Aussois, pp. 493–498.

Storek, H., Brauer, H., 1980. Reibungsdruckverlust der adiabaten Gas-Fluessigkeits-Stroemung. VDI Forschungsheft, No. 599.

Sutton, G.W., Hurwitz, H., Poritsky, H., 1962. Electrical and pressure losses in a magnetohydrodynamic channel due to end current loops. Trans. AIEE, Part I 80, 687–695.

Szekely, J., 1979. Fluid Flow Phenomena in Metals Processing. Academic Press, New York.

Tanatugu, N., Fujii-E, Y., Suita, T., 1972. Electrical conductivity of liquid metal two-phase mixture in bubbly and slug flow regime. J. Nucl. Sci. Technol 9, 753–755.

Thibault, J.-P., 1986. Modelling of two-phase magnetohydrodynamic flows. In: Ninth International Conference on MHD Electrical Power Generation, Tsukuba.

Thibault, J.-P., Mihalache, G., 1997. LMMHD two-phase flow: experiments in a mercury–air MHD flow. In: Proceedings of the Third International Conference on Transfer Phenomena in Magnetohydrodynamic and Electroconducting Flows, Aussois, 517–522.

van Wijngarden, L., 1972. One-dimensional flow of liquids containing small gas bubbles. Ann. Rev. Fluid Mech 4, 369–396.

Yakhot, A., Branover, H., 1982. An analytical model of a two-phase liquid metal magnetohydrodynamics generator. Phys. Fluids 25, 446–449.

Yonas, G., 1967. Measurements of drag in a conducting fluid with an aligned field and large interaction parameter. J. Fluid Mech 30, 813–821.

Zuber, N., Findlay, J.A., 1965. Average volumetric concentration in two-phase flow systems. J. Heat Transfer 87, 453–468.